www.rericjournal.ait.ac.th

Numerical Study of Waste Heat Recovery from Tunnel Kiln Utilized to Produce Rare Earth Phosphor

Linsheng Wei*[1], Liangyin Guo*, Zhang Yafang*, Hu Zhaoji* and Tan Zhihong*

Abstract – An indirect heat recovery method is adopted to recover waste heat from tunnel kiln supplied by electricity utilized to produce rare earth phosphor. To ensure the quality of products and the life of tunnel kiln, a water tank is installed surrounding the cooling region of tunnel kiln as a heat exchanger. Meanwhile, a computational fluid dynamics model is developed to estimate and optimize the performance of this waste heat recovery. The predicted temperatures are in good agreement with measured results, and the error is within a reasonable range. In addition, a relationship between the inlet mass flow rate and the inlet water temperature is obtained in terms of desired outlet water temperature. Using water tank as a heat exchanger is an effective and reasonable method to recover waste heat of tunnel kiln utilized to further process of rare earth phosphor. The 4443 kg standard coal would be saved a year when inlet water temperature is 285 K.

Keywords – Computational fluid dynamics, heat recovery, rare earth phosphor, tunnel kiln, water tank.

1. INTRODUCTION

China has an abundance of rare earth resources, and tunnel kiln supplied by electricity is widely applied in rare earth phosphor production. The loss of heat in a tunnel kiln is mainly attributed to hot flue gas and kiln shell [1]–[6]. Therefore, waste heat recovery from hot gases and hot kiln surfaces is known as a potential way to reduce energy consumption of tunnel kiln. There are two principal methods of waste heat recovery: direct extraction of hot flue gas and indirect heat exchange through kiln surfaces in cooling region. The former method has been fully researched [7]–[9]. However, there are some problems for direct extraction of hot flue gas in a tunnel kiln supplied by electricity as follows:

1) More energy would be consumed, which would greatly impact the temperature of reaction region so that reduce the product quality.

2) It is not practical because there is little use for the waste heat on site and its transportation cost is too expensive.

Therefore, indirect heat recovery is regarded as a more effective and reasonable method to recover waste heat of tunnel kiln.

With the development of computer science and technology, Computational Fluid Dynamics (CFD) has been extensively used in many fields of industrial applications including heat recovery from kiln [10]–[17]. A dynamic model, which described the behavior of a rotary kiln for waste incineration, was presented to follow large variations in process conditions and to be of practical value from a control point of view [18]. Some numerical heat transfer models were employed for estimating the performance of radiant heat recovery exchangers applied to rotary kilns supplied by fuel combustion for cement production [19]–[21]. A mathematical model was developed to investigate important parameters variables along the cooling region of tunnel kiln and to optimize waste heat recovery system in a brick making process supplied by coal combustion [22]. To sum up, numerical method which used to analysis the waste heat recovery from kiln has been demonstrated as an effective approach.

The quality of rare earth phosphor material made in China has reached the top level of world. The further processing of rare earth phosphor material is a high energy-consumption process. Unfortunately, the energy consumption in this process is almost neglected. The energy efficiency of tunnel kiln is very low, which is utilized to further process of rare earth phosphor material. Only about 5 % is effectively used, and the rest is lost according to statistics. The aim of this paper is to investigate the heat recovery from a tunnel kiln supplied by electricity which is utilized to rare earth phosphor production, and to obviously reduce the energy consumption of this process.

2. METHODS

2.1 Experimental Set-up

The tunnel kiln supplied by electricity is divided into preheating region, reaction region, and cooling region. The main work of this paper is to study the waste heat recovery from the cooling region, which is composed of the extension section, the connection section, and the exit section, as shown in Figure 1.

In rare earth phosphor production progress, crucibles are filled of raw material at first, and then move with stripper plate in tunnel kiln from tunnel inlet to outlet. The components of the rare earth raw material are very complex including Y_2O_3, Eu_2O_3, CeO_2, Tb_4O_7 and so on. Its physical properties is quite similar to Al_2O_3, whose density, specific heat capacity, thermal conductivity and mass are 3970 kg/m^3, 0.992 kJ/kg·K, 16.72 W/m·K, 1.0 kg, respectively. The crucible is made of aluminum oxide ceramics, whose density, specific heat capacity, thermal conductivity and mass are 3900

*School of Resources Environment and Chemical Engineering, Nanchang University, Nanchang 330031, China.

[1]Corresponding author: Tel: + 86 150 700 741 05.
E-mail: weilinsheng@ncu.edu.cn

kg/m^3, 0.992 kJ/kg·K, 8.352 W/m·K, 0.5 kg, respectively. The material of stripper plate is mullite, whose density, specific heat capacity, thermal conductivity and mass are 3160 kg/m^3, 1.1 kJ/kg·K, 4.443 W/m·K, 2 kg , respectively.

(a) Tunnel inlet

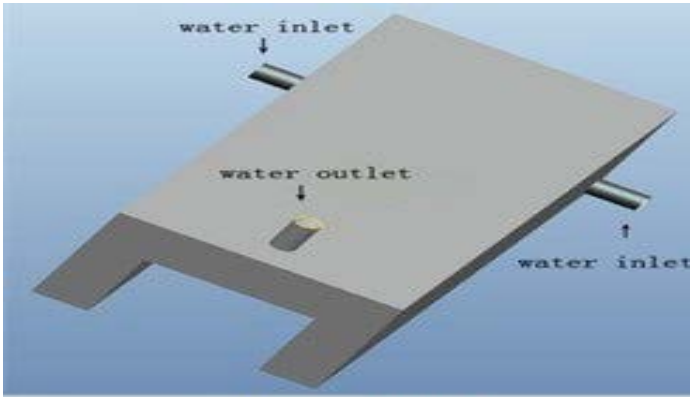

(b) Water Tank

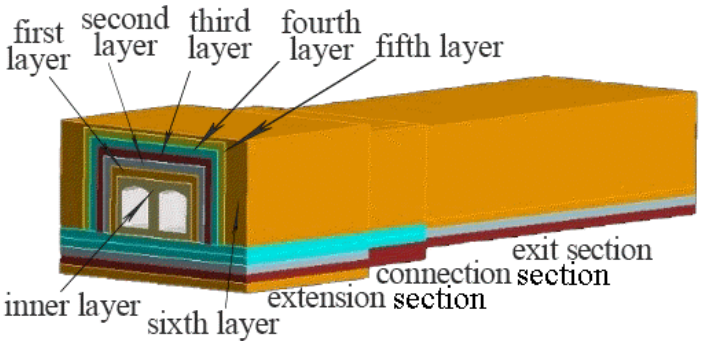

(c) Cooling Region Model

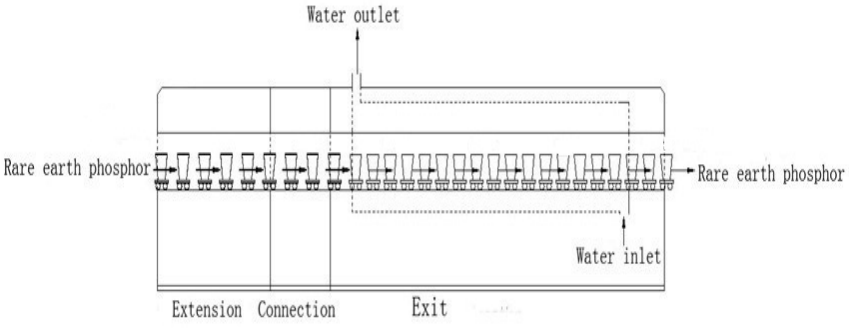

(d) Cooling Region of Tunnel Kiln

Fig. 1. Experimental set-up.

Plenty of insulation bricks are installed around the tunnel kiln in order to reduce energy loss. The structure of insulation layer in the cooling region is shown in Figure 1 (c). It can be seen that the structures of insulation layer in different part of cooling region are not the same. In extension section, the insulation layer is composed of seven layers, their materials and properties are shown in Table 1. Compared with the extension section, the difference is only that the connection section is lack of the first layer, and there is no the first and second layer in the exit section.

The temperature of rare earth phosphor at outlet of preheating region is about 1600 K and then increases to about 1800 K in the reaction region. Water tank is arranged at the exit section of cooling region in order to ensure the temperature of reaction region, and thus guarantee the product quality and life of tunnel kiln.

The temperature in tunnel kiln was measured by some high-temperature thermocouples (WRR-130), which were installed on the outer surface of the insulation layer of tunnel kiln. The hot electrode of thermocouples penetrated the insulation layer and then reaches the inner channel of the tunnel kiln. The actual temperature was shown via control panel.

Table 1. The material properties of extension section.

Layers	Material	Density kg/m^3	Specific heat capacity J/(kg·K)	Thermal conductivity W/(m·K)
Inner layer	Alumina hollow brick	1300	861	0.83
First layer	Mullite brick	800	1000	1.03
Second layer	Mullite brick	800	1000	1.18
Third layer	High alumina bricks	800	1093	2.245
Fourth layer	Light high alumna	600	1024	0.468
Fifth layer	Light high alumna	600	1024	0.433
Sixth layer	Ordinary aluminum-silicate refractor fiber	300	1240	0.0474

2.2 Numerical Simulation

The simplified experimental devices and the precise equations make it possible to study the heat transfer in the tunnel kiln. In this paper, some assumptions are made as follows:

1) The physical properties of crucible, stripper plate, and raw material are constant.

2) The variation of gas flow rate in the axial direction and the effect of air humidity are not taken into account in the model in order to simplify the calculation.

3) Heat is transferred between the gas and products mainly by natural convection and radiation.

4) Steady state working conditions.

Based on the actual structure and the simplified principles, the physical model is created as shown in Figure 1(c). Finite volume method is employed to solute equations of mass, momentum, and heat energy conservation. These equations are as follows:

Continuity

$$\frac{\partial \rho}{\partial t}+\frac{\partial}{\partial x_i}(\rho \vec{u_i})=S_C \tag{1}$$

Momentum

$$\frac{\partial(\rho u_i)}{\partial t}+\frac{\partial(\rho u_i u_j)}{\partial x_j}=-\frac{\partial p}{\partial x_i}+\frac{\partial \sigma_{ij}}{\partial x_j}+S_M \tag{2}$$

$$\sigma_{ij}=\mu(\frac{\partial u_3}{\partial x_j}+\frac{\partial u_j}{\partial x_i})-\frac{2}{3}\mu\delta_{ij}\frac{\partial u_i}{\partial x_i} \tag{3}$$

Energy

$$\frac{\partial(\rho E)}{\partial t}+\frac{\partial(u_i(\rho E+p))}{\partial x_i}=\frac{\partial}{\partial x_i}(k\frac{\partial T}{\partial x_i}+u_j\sigma_{ij})+S_E \tag{4}$$

3. RESULTS AND DISCUSSION

3.1 Axial Temperature Distribution without Water Tank

Figure 2 shows axial temperature distribution of rare earth phosphor in cooling region when the water tank is not installed. Obviously, it can be seen that the temperature steadily decreases along direction of movement, meanwhile the simulated and measured results agree very well with each other. In addition, the energy which is emitted through the tunnel kiln surface is 20687 W according the calculation of the simulation results. It shows that a lot of potential energy can be recycled.

3.2 Influence of Water Tank Length

In the study, the outlet water temperature is one of the most significant characteristics. In the numerical model, outlet water temperature can be calculated via equation 5.

$$\overline{T_t}=\frac{\int_A(\rho T_t \mid \vec{v}\cdot\hat{n}\mid)dA}{\int_A(\rho \mid \vec{v}\cdot\hat{n}\mid)dA} \tag{5}$$

Figure 3 shows outlet water temperature as function of water tank length at various flow rates when inlet water temperature is 290 K. It can be observed that the outlet water temperature slightly increases with

increasing water tank length. The simulated outlet water temperature increases from 347 K to 353 K at flow rate of 0.0576 m^3/h. This is to say that water tank length has little effect on the outlet water temperature.

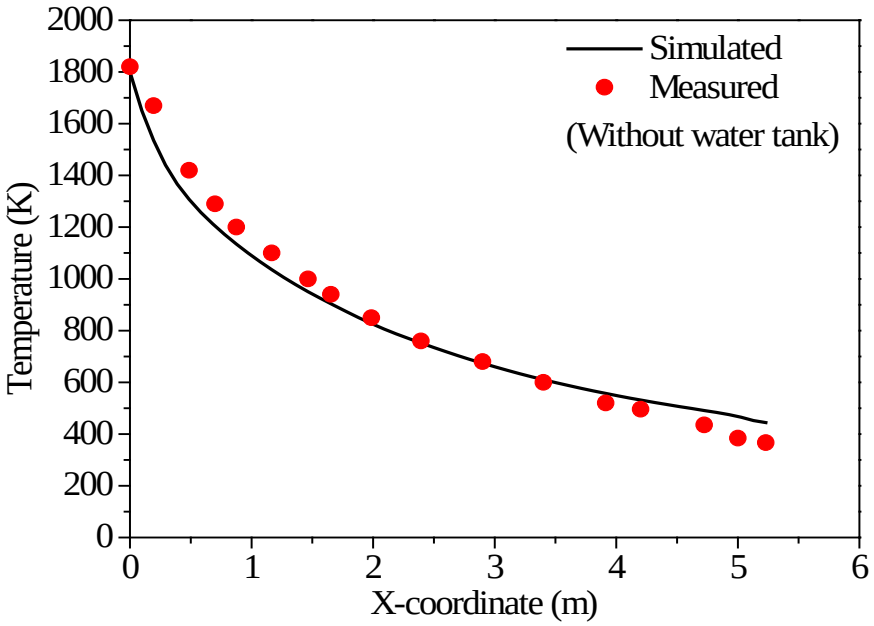

(a)

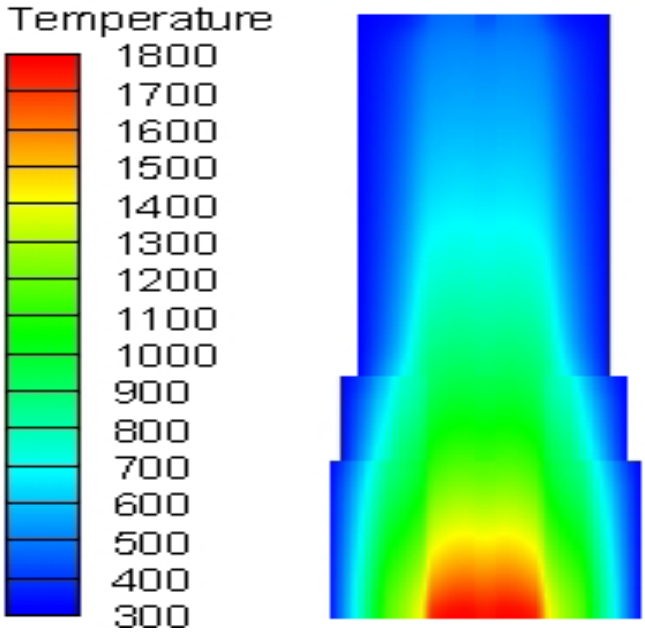

(b)

Fig. 2. Axial temperature distribution of rare earth phosphor in cooling region without water tank.

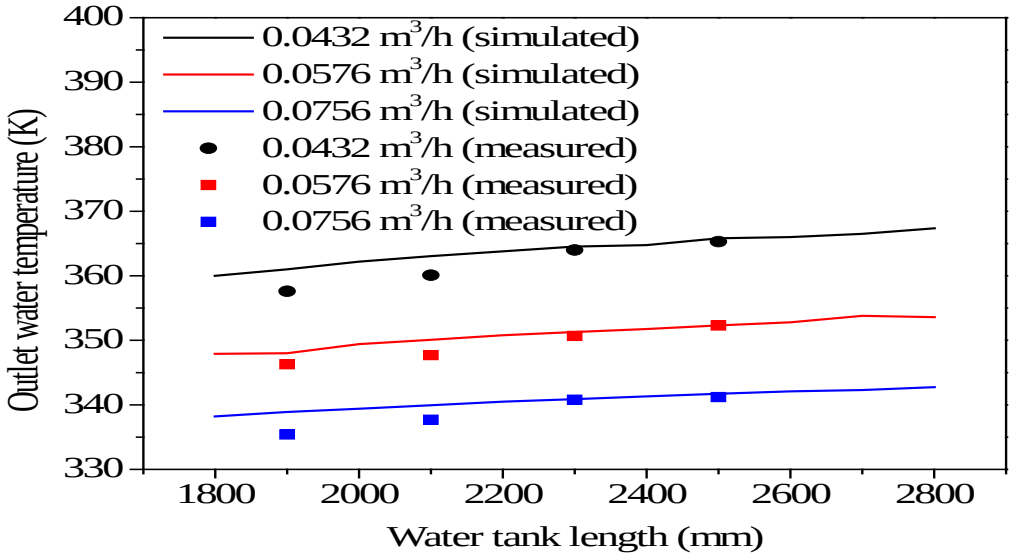

Fig. 3. Outlet water temperature variation with different water tank length at various flow rates.

3.3 Influence of Flow Rate Inlet Water Temperature

For simplification, water tank length is set to 2.0 m in following section because water tank length has little influence on outlet water temperature when water tank length increases from 1.8 m to 2.8 m. The factory is located in Ganzhou, Jiangxi province of China, inlet water temperature ranges from about 270 K to 300 K all the year round. Therefore, the variation of inlet water temperature is taken into account in the simulation. Figure 4 depicts the outlet water temperature variation with different inlet water flow rate and temperatures when the water tank length is 2.0 m. It can be easily observed that outlet water temperature increases with increasing inlet water temperature and decreasing inlet water flow rate. The outlet water temperature reaches the highest value of 368.5 K at inlet water flow rate of 0.0432 m^3/h and inlet water temperature of 300 K.

Outlet water temperature is desired to reach approximately 343 K, the heat water can be used to wash the rare earth phosphors obtained in tunnel kiln. In order to gain desired outlet water temperature, a function of third order between the inlet mass flow rate V (g/s) and the inlet water temperature T (K) is obtained as shown in Figure 5 as follows:

$$V = -3054.428 + 33.7541T - 0.12451T^2 + 0.000154017T^3 \quad (6)$$

The inlet water flow rate can be determined according inlet water temperature via Equation 6 in practical rare earth phosphor production process.

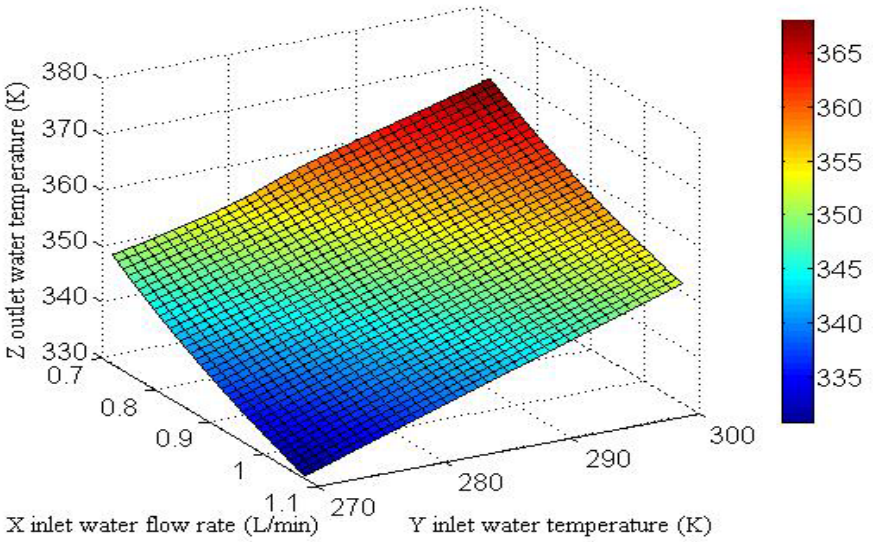

Fig. 4. Outlet water temperature variation with different inlet water flow rates and temperatures.

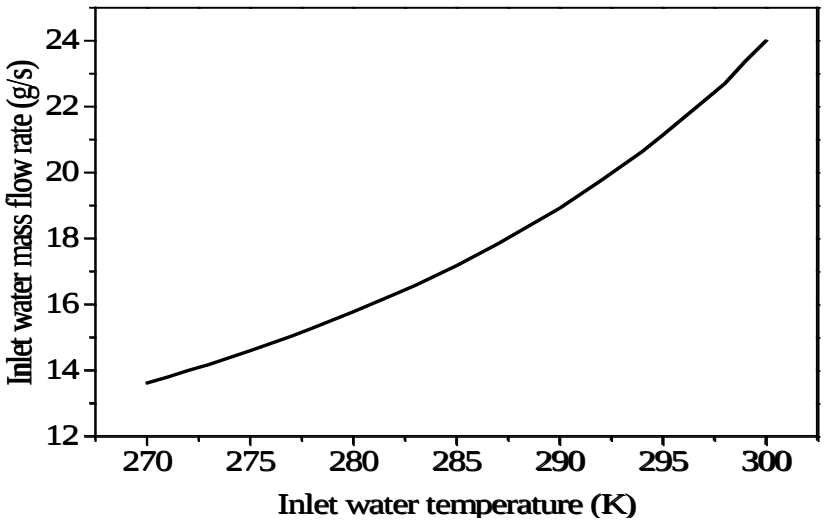

Fig. 5. Optimization relationship for inlet water temperature and inlet water flow rate.

3.4 Axial Temperature Distribution with Water Tank

The installation of water tank has little effect on rare earth phosphor temperature, and furthermore has no effect on the quality of products and the life of tunnel kiln as shown in Figure 6. Thus, water tank installed around the cooling region of tunnel kiln as a heat exchange is a feasible way to recovery waste heat. The simulated results and the measured results agree very well with each other, which shows the model is enough reliable.

The inlet water flow rate is 0.062 m^3/h when inlet water temperature is 285 K in terms of the relationship of Equation 6. The heat water of 1468 kg is obtained every day at desired temperature of 343 K. The power transferred to water is 4070 W according the optimization results. The energy of 1.3×10^{11} J would be saved a year, and the equivalent quantities of standard coal is 4443 kg a year. This shows that using water tank as a heat exchanger is an effective and reasonable method to recover waste heat of tunnel kiln utilized to further process of rare earth phosphor.

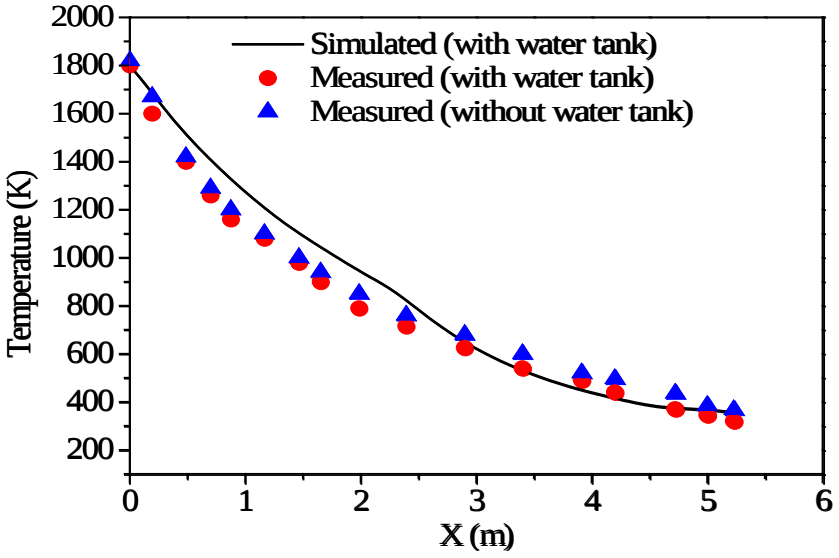

(a)

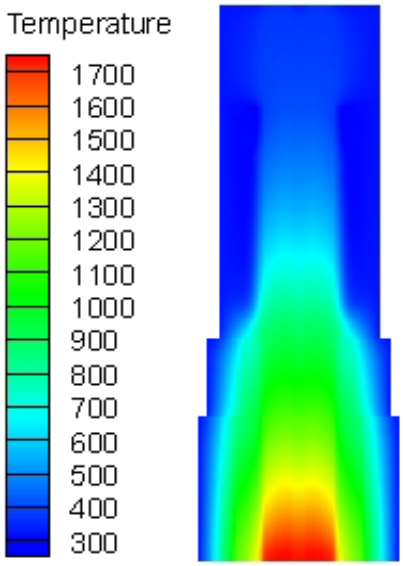

(b)

Fig. 6. Axial temperature distribution of rare earth phosphor in cooling region with water tank.

4. ERROR ANALYSIS

In order to test the accuracy of numerical simulation results, error analysis is necessary. The simulation errors are mainly consists of physical modelling errors, discretization errors, computer round-off errors and iterative convergence errors.

4.1 Physical Modelling Errors

Physical modelling errors arise from mathematical model form assumptions, boundary conditions and initial conditions. In this simulation, the adopted initial conditions and boundary conditions are close to the actual working conditions. These assumptions and simplifications made in the simulation are reasonable, and their effects are too small to be considered.

4.2 Discretization Errors

Discretization errors are defined as the difference between exact solution to the discrete equations and analytical solution to the partial differential equations. These errors occur from the algebraic expressions of the governing flow equations and other physical models in a discrete domain of space and time. This type of error arises in all numerical methods. Therefore discretization errors are also termed as numerical errors. It is related to the approximate representation of a parameter which varies continuously in space by some polynomial function for the variation across a mesh cell. The discretization errors will tend to zero when the number of grid points increases and the size of the grid spacing tends to zero. As the mesh is refined, the solution should become less sensitive to the grid spacing and approach the continuum solution. This is grid convergence. In this simulation, the size of the grid spacing is small enough.

4.3 Computer Round-Off Errors

Computer round-off errors occur when exact solution cannot be extracted from discrete equations. They result from precision floating-point numbers which can only represent discrete points on the real number line. These errors are unimportant, but sometimes they cause major inaccuracy or may prevent convergence. In this simulation, the computer round-off errors are minimized by double precision method.

4.4 Iterative Convergence Errors

Iterative convergence errors exist because the iterative methods used in simulation must have a stopping point eventually. The time consuming iterations are generally truncated close to the final solution. In this simulation, the iterative convergence errors reduce with increasing iterative computing time.

4.5 The Inspection of Simulation Errors

In order to further test the error of the model, the relative simulation error is introduced, which is calculated by equation as follow:

$$\varepsilon = \frac{|C - M|}{M} \times 100\% \tag{7}$$

Figure 7 shows the distribution of the relative error between simulation and measurement results. It can be seen that the relative simulation error is enough small, and only a few errors are greater than 15 %. The average relative simulation errors without water tank and with water tank are 7.71 % and 8.82 %, respectively. The maximum average relative error between simulation and measure is less than 10 %, which is within a reasonable range.

In summary, the results of error analysis indicate that the CFD model is feasible and reliable.

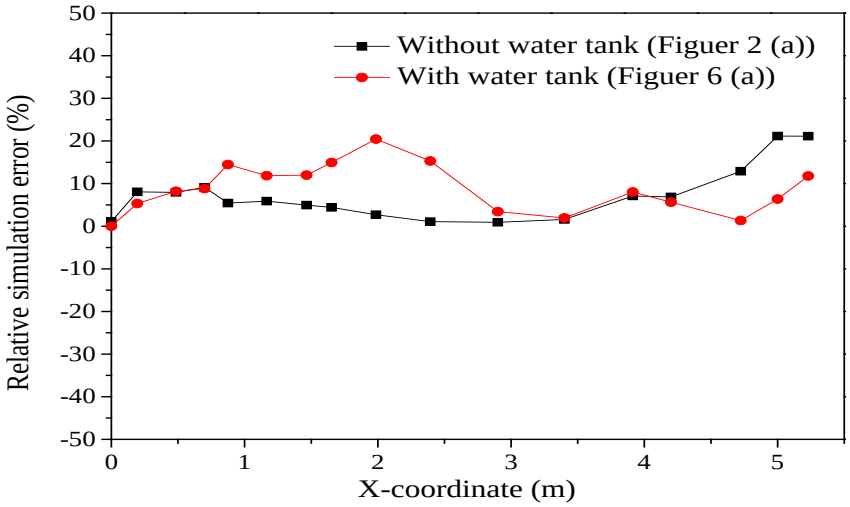

Fig. 7. Distribution of the error between simulation and measurement results.

5. CONCLUSIONS

A water tank as a heat exchanger is installed in cooling region of tunnel kiln utilized to further process of rare earth phosphor in order to recover waste heat of tunnel kiln. Meanwhile, a CFD model is developed to estimate and optimize the performance of this indirect heat recovery.

1) The numerical simulation results are in good agreement with the experimental data. The maximum average relative error between the simulation and experiment is 8.82 %, which is within a reasonable range. The numerical simulation method is very simple and suitable for this heat recovery application.

2) The outlet temperature increases with increasing inlet water temperature and decreasing water flow rate. In order to gain desired outlet water temperature, a relationship between the inlet mass flow rate and the inlet water temperature is obtained. And the inlet water flow rate can be determined according inlet water temperature in practical rare earth phosphor production process.

3) Using water tank as a heat exchanger is an effective and reasonable method to recover waste heat of tunnel kiln utilized to further process of rare earth phosphor. The 4443 kg standard coal would be saved a year when inlet water temperature is 285 K. In addition, the quality of products and the life of tunnel kiln are guaranteed.

NOMENCLATURE

CFD Computational Fluid Dynamics

Equations 1 to 4:

ρ	density, kg/m^3
t	time, s
u_i	x_i-direction velocity component, m/s
σ_{ij}	stress tensor
p	static pressure, pa
μ	dynamic viscosity, N·s/m^2
k	thermal conductivity, W/(m·K)
T	temperature, K
E	total energy per unit mass, J
S_C	mass source term
S_M	momentum source term
S_E	energy source term

Equation 5:

T_t	outlet water temperature, K
A	area of the outlet, m^2
$\vec{v}$	velocity vector
ρ	fluid density, kg/m^3
$\hat{n}$	a unit vector normal to the surface

Equation 7:

C	simulated result
M	measured result
ε	relative simulation error

ACKNOWLEDGEMENT

The project was supported by the Science and Technology Pillar Program of Jiangxi Province, China (20122BBG70069-1).

REFERENCES

[1] Chakrabarti B.K., 2002. Investigations on heat loss through the kiln shell in magnesite dead burning process: a case study. *Applied Thermal Engineering* 22: 1339-1345.

[2] Madlool N.A., Saidur R., Hossain M.S. and Rahim N.A., 2011. A critical review on energy use and savings in the cement industries. *Renewable and Sustainable Energy Reviews* 15: 2042-2060.

[3] Shi D.L., Vargas W.L. and McCarty J.J. 2008.

Heat transfer in rotary kilns with interstitial gases. *Chemical Engineering Science* 63: 4506-4516.

[4] Khurana S., Banerjee R. and Gaitonde U., 2002. Energy balance and cogeneration for a cement plant. *Applied Thermal Engineering* 22: 485-494.

[5] Karamarković V., Marašsević M., Karamarković R. and Karamarković M., 2013. Recuperator for waste heat recovery from rotary kilns. *Applied Thermal Engineering* 54: 470-480.

[6] Karellas S., Leontaritis A.-D., Panousis G., Bellos, E. and Kakaras E., 2013. Energetic and exergetic analysis of waste heat recovery systems in the cement industry. *Energy* 58: 147-156.

[7] Casci C., Angelino G., Ferrari P., Gaia M., Giglioli G. and Macchi E., 1981. Heat-recovery in a ceramic kiln with an organic rankine-cycle engine. *Journal of Heat Recovery Systems* 1: 125-131.

[8] Herz F., Mitov I., Specht E. and Stanev R., 2012. Influence of operational parameters and material properties on the contact heat transfer in rotary kilns. *International Journal of Heat and Mass Transfer* 55: 7941-7948.

[9] Atmaca A. and R. Yumrutaş. 2014. Analysis of the parameters affecting energy consumption of a rotary kiln in cement industry. *Applied Thermal Engineering* 66: 435-444.

[10] Sogut Z., Oktay Z. and Karakoc H., 2010. Mathematical modeling of heat recovery from a rotary kiln. *Applied Thermal Engineering* 30: 817-825.

[11] Volkov V.Y., Belova O., Krutikov A. and Skibin A., 2013. A coolant flow simulation in fast reactor wire-wrapped assembly. *Thermal Engineering* 60: 429-433.

[12] Semchenkov Y.M. and V. Sidorenko. 2011. Prospects for development of nuclear power stations equipped with VVER reactors. *Thermal Engineering* 58: 361-369.

[13] Ginsberg T. and M. Modigell. 2011. Dynamic modelling of a rotary kiln for calcination of titanium dioxide white pigment. *Computers and Chemical Engineering* 35: 2437-2446.

[14] Manju M.S. and S. Savithri. 2012. Three dimensional CFD simulation of pneumatic coal injection in a direct reduction rotary kiln. *Fuel* 102: 54-64.

[15] Oba R., Possamai T.S. and Nicolau V.P., 2014. Thermal analysis of a tunnel kiln used to produce roof tiles. *Applied Thermal Engineering* 63: 59-65.

[16] Saidur R., Hossain M.S., Islam M.R., Fayaz H. and Mohammed H.A., 2011. A review on kiln system modeling. *Renewable and Sustainable Energy Reviews* 15: 2487-2500.

[17] Mujumdar S.K. and V.V. Ranade. 2008. CFD modeling of rotary cement kilns. *Asia-Pacific Journal of Chemical Engineering* 3: 106-118.

[18] Rovaglio M., Manca D. and Biardi G., 1998. Dynamic modeling of waste incineration plants with rotary kilns: comparisons between experimental and simulation data. *Chemical Engineering Science* 53: 2727-2742.

[19] Caputo A.C., Pelagagge P.M. and Salini P., 2011. Performance modeling of radiant heat recovery exchangers for rotary kilns. *Applied Thermal Engineering* 31: 2578-2589.

[20] Stadler K.S., Poland J. and Gallestey E., 2011. Model predictive control of a rotary cement kiln. *Control Engineering Practice* 19: 1-9.

[21] Yin H.C., Zhang M. and Liu H., 2014. Numerical simulation of three-dimensional unsteady granular flows in rotary kiln. *Powder Technology* 253: 138-145.

[22] Kaya S., Küçükada K. and Mançuhan E., 2008. Model-based optimization of heat recovery in the cooling zone of a tunnel kiln. *Applied Thermal Engineering* 28: 633-641.